Efimov resonance position near a narrow Feshbach resonance in a ^{6}Li - ^{133}Cs mixture

Ang Li ⬤,[1] Yaakov Yudkin,[1] Paul S. Julienne,[2] and Lev Khaykovich ⬤[1]

[1]*Department of Physics, QUEST Center and Institute of Nanotechnology and Advanced Materials,*
Bar-Ilan University, Ramat-Gan 5290002, Israel
[2]*Joint Quantum Institute, University of Maryland and NIST, College Park, Maryland 20742, USA*

In the vicinity of a narrow Feshbach resonance Efimov features are expected to be characterized by the resonance's properties rather than the van der Waals length of the interatomic potential. Although this theoretical prediction is well established by now, it still lacks experimental confirmation. Here, we apply our recently developed three-channel model [Y. Yudkin and L. Khaykovich, Efimov scenario for overlapping narrow Feshbach resonances, Phys. Rev. A **103**, 063303 (2021)] to the experimental result obtained in a mass-imbalanced ^{6}Li - ^{133}Cs mixture in the vicinity of the narrowest resonance explored to date [J. Johansen, B. J. DeSalvo, K. Patel, and C. Chin, Testing universality of Efimov physics across broad and narrow Feshbach resonances, Nat. Phys. **13**, 731 (2017)]. Our analysis suggests that the observed position of the Efimov resonance is dictated mainly by the resonance physics while the influence of the van der Waals tail of the interatomic potential is minor. We show that the resonance position is strongly influenced by the presence of another Feshbach resonance which significantly alters the effective background scattering length at the narrow resonance position.

I. INTRODUCTION

The Efimov effect in ultracold atoms emerges when the scattering length a greatly exceeds the van der Waals length r_{vdW} of the interatomic potential [1]. The resonantly enhanced two-body interactions give rise to an infinite ladder of three-body bound states separated by a universal scaling factor. Thus, to fully determine the three-body spectrum it suffices to do so for a single state. Moreover, as the state's dependence on a is described by a universal function, a single parameter is enough to define the entire spectrum. For this matter it is convenient to choose the scattering length value a_- at which the ground state of the Efimov state meets the free-atom continuum. Experimentally, this is the best studied parameter to date [2–4].

It was predicted that a_- depends on the underlying two-body collisional resonance strength which is conveniently characterized by a dimensionless parameter s_{res}. A collisional Feshbach resonance occurs when the free atoms in an open channel are coupled to a nearly degenerate two-body bound state in a closed channel [5]: For strong coupling with $s_{res} \gg 1$ (also known as the broad resonance regime) a_- is universally related to r_{vdW} [2,3]. When the coupling weakens, a_- deviates from this universality and, instead, tends to be dictated by the effective range of the Feshbach resonance for $s_{res} \ll 1$. The latter regime can be described by a simplified theory with a short-range potential tuned to have the same effective range as the true interaction potential [6].

Experimental studies of narrow resonances are difficult due to the extreme magnetic-field stability requirement. The difficulties are twofold. First, the position of the Efimov resonance is predicted to be pushed towards higher scattering length values as compared to broad resonances which follow the Efimov–van der Waals universality. Second, narrow resonances are usually literally narrow, i.e., they are narrow functions of the magnetic field, which causes large changes in the scattering length over tiny variations of the magnetic field. The combination of these two factors renders an unrealistically tough requirement on the magnetic-field stability, and hence this demanding regime was rarely approached experimentally [7,8]. The narrowest resonance studied to date is in the ^{6}Li - ^{133}Cs mixture [9].

The few-body aspects of heteronuclear mixtures attracted significant interest in the last decade, both theoretical [10–20] and experimental [21–28]. The ^{6}Li - ^{133}Cs mixture is the most extreme mass-imbalanced system in which Efimov features were observed to date making it favorable for the attempt to reveal the few-body physics at a narrow Feshbach resonance. In contrast to homonuclear systems, where the large universal scaling factor makes the observations of two consecutive Efimov resonances challenging [29], the large mass ratio in the Efimov favorable heavy-heavy-light scenario was predicted to decrease the scaling factor significantly [10]. The Efimov physics in the ^{6}Li - ^{133}Cs mixture has been the subject of intense experimental investigation in the vicinity of two broad Feshbach resonances and the decreased scaling factor was confirmed [25–28]. This motivated the attempt to look for Efimov features in the vicinity of a narrow Feshbach resonance despite the fact that no theoretical prediction is available in this region [9].

Indeed, the position of the Efimov resonance was revealed at a larger scattering length as compared to the position predicted by the Efimov–van der Waals universality and measured in the vicinity of broad resonances [9]. As the model

of Ref. [6], in its original form, is limited to three identical bosons, this result remains theoretically unexplored. Nevertheless, developing a suitable theory can clarify several interesting aspects of the three-body physics at a narrow resonance. For example, how important is the van der Waals tail of the real interatomic potential compared to the resonance physics? And what is the influence of a nearby overlapping Feshbach resonance?

Here we consider these questions by extending our recently developed three-channel theory to mass-imbalanced mixtures and applying it to the experimentally relevant resonances in the ^{6}Li-^{133}Cs mixture. We show that the position of the Efimov resonance is well captured by this theory if the overlapping Feshbach resonances are properly taken into account. Based on this result we can place the upper bound for the contribution of the finite range of the interatomic potential (i.e., the van der Waals length) to the position of the Efimov resonance. Unfortunately, the lack of other experimental results under similar conditions prohibits further benchmarking of our model.

Finally, we note that there is a growing effort to incorporate realistic multichannel two-body interactions in few-body theories to improve their performance when applied to real systems [8,30–32]. Our approach supports the necessity of these efforts.

II. MODEL HAMILTONIAN

Inspired by the two-channel model [6,33,34], we develop a suitable model step by step, starting from an open channel of free atoms. By considering a noninteracting open channel (zero background scattering) the short-range physics is neglected. The resonant two-body interactions are modeled by coupling the open channel to a closed molecular channel which is detuned by a magnetic-field-dependent binding energy. The weakly coupled limit (narrow resonance) leads to a large effective range r_e which significantly exceeds $r_{\rm vdW}$ [34]. More resonances can be included by coupling the open channel to additional closed channels [35].

We consider a ^{6}Li-^{133}Cs mixture where both atoms are prepared in their respective absolute ground states (*aa* channel). At 893 G there is a narrow Feshbach resonance which, according to coupled-channel calculations using the model of Ref. [36], features a large and negative effective range at the resonance's position ($r_e = -1541a_0$, where a_0 is the Bohr radius). As the van der Waals length of the Li-Cs interaction potential is $r_{\rm vdW} = 44.8a_0$, the narrow resonance criterion is well satisfied: $|r_e| \gg r_{\rm vdW}$ or, alternatively, $s_{\rm res} = 0.0509 \ll 1$. Moreover, $a_{bg} = -30a_0$ justifies the assumption of negligible background scattering [36–38]. However,

another Feshbach resonance at 843 G is expected to play an important role. This resonance is of intermediate character, being neither broad nor narrow. As is shown below, it overlaps with the narrow resonance and strongly alters the local background scattering in the latter's vicinity. Taking into account the 843-G resonance is essential to reveal the predictive power of our three-channel model.

We start with the most generic case of three distinguishable atomic species (labeled $i = 1, 2, 3$) with masses m_i. Each atom pair can form a molecule in either of two closed channels $\nu = 1, 2$. We define creation operators of atoms, $\hat{a}^\dagger_{\vec{q},i}$, and of molecules, $\hat{b}^\dagger_{\vec{q},i,\nu}$, where $\vec{q}$ denotes the particle's momentum. The index i in $\hat{b}^\dagger_{\vec{q},i,\nu}$ labels the atom *not* part of the molecule. The operators satisfy standard commutation relations. The conversion of two atoms $i \neq j$ to a molecule $k \neq i, j$ in channel ν is most generally described by the term

$$\delta(\vec{q}_1 - \vec{q}_2 - \vec{q}_3)\hat{b}^\dagger_{\vec{q}_1,k,\nu}\hat{a}_{\vec{q}_2,i}\hat{a}_{\vec{q}_3,j}, \tag{1}$$

where $\delta(\vec{q}_1 - \vec{q}_2 - \vec{q}_3)$ signifies momentum conservation.

The total Hamiltonian consists of a bare atomic, a bare molecular, and an interaction term:

$$\hat{H} = \hat{H}^{\rm (at)} + \hat{H}^{\rm (mol)} + \hat{H}^{\rm (int)}. \tag{2}$$

The bare atomic term is made of three parts, one for each species:

$$\hat{H}^{\rm (at)} = \sum_{i=1}^3 \hat{H}^{\rm (at)}_i, \tag{3a}$$

$$\hat{H}^{\rm (at)}_i = \int \frac{d^3q}{(2\pi)^3} \frac{\hbar^2 q^2}{2m_i} \hat{a}^\dagger_{\vec{q},i}\hat{a}_{\vec{q},i}. \tag{3b}$$

The bare molecular term is made of six parts, one for each pair (i) and each channel (ν):

$$\hat{H}^{\rm (mol)} = \sum_{i=1}^3 \sum_{\nu=1}^2 \hat{H}^{\rm (mol)}_{i,\nu}, \tag{3c}$$

$$\hat{H}^{\rm (mol)}_{i,\nu} = \int \frac{d^3q}{(2\pi)^3} \left(\frac{\hbar^2 q^2}{2M_i} + E_{i,\nu}\right)\hat{b}^\dagger_{\vec{q},i,\nu}\hat{b}_{\vec{q},i,\nu}, \tag{3d}$$

where the mass of a molecule is $M_i = (m_j + m_k)$ and the energy detuning from the open channel is $E_{i,\nu} = \mu_{i,\nu}(B_{i,\nu} - B)$ with $\mu_{i,\nu}$ the differential magnetic moment and $B_{i,\nu}$ the bare resonance position. Finally, the interaction term also consists of six parts:

$$\hat{H}^{\rm (int)} = \sum_{k=1}^3 \sum_{\nu=1}^2 \hat{H}^{\rm (int)}_{k,\nu}, \tag{3e}$$

$$\hat{H}^{\rm (int)}_{k,\nu} = \frac{\Lambda_{k,\nu}}{2} \sum_{i,j \neq k} \int \frac{d^3q_1}{(2\pi)^3} \int \frac{d^3q_2}{(2\pi)^3} \left[\hat{b}^\dagger_{\vec{q}_1,k,\nu}\hat{a}_{\vec{q}_2+\frac{\vec{q}_1}{2},j}\hat{a}_{-\vec{q}_2+\frac{\vec{q}_1}{2},i} + \hat{a}^\dagger_{-\vec{q}_2+\frac{\vec{q}_1}{2},i}\hat{a}^\dagger_{\vec{q}_2+\frac{\vec{q}_1}{2},j}\hat{b}_{\vec{q}_1,k,\nu}\right], \tag{3f}$$

where the factor of 1/2 avoids double counting. Note that we assume zero direct coupling between the two closed channels $\nu = 1$ and 2. Without loss of generality, this coupling can be

diagonalized by introducing a dressed basis in which interactions are absorbed by the energy shifts. A more rigorous approach considered in Ref. [35] shows that this coupling

adds an additional free parameter to the system which remains redundant when the other parameters are fixed by the two-body observables. Indirect coupling through the common continuum remains intact.

III. THREE DISTINGUISHABLE PARTICLES

A. Two-body sector

Since there are three distinct atomic species there are three two-body sectors $k = 1, 2, 3$. However, all three are permutations of each other. The kth two-body sector is described by the Schrödinger equation $(\hat{H} - E)|\psi_k^{(2B)}\rangle = 0$ and the (center-of-mass frame) two-body ansatz is

$$\left|\psi_k^{(2B)}\right\rangle = \left(\sum_\nu \beta_{k,\nu}\hat{b}_{\vec{q}=0,k,\nu}^\dagger + \int \frac{d^3q}{(2\pi)^3}\alpha_k(\vec{q})\hat{a}_{\vec{q},i}^\dagger\hat{a}_{-\vec{q},j}^\dagger\right)|0\rangle,$$
(4)

where $i \neq j \neq k \neq i$. Scattering properties, in particular the scattering length a_k and the effective range $r_{e,k}$, are derived from the positive-energy solution $E = \hbar^2 q_k^2/2\mu_k > 0$, while for $E = -\hbar^2(\lambda_k^D)^2/2\mu_k < 0$ the dimer binding energy is found. Here, $\mu_k = m_i m_j/(m_i + m_j)$ is the reduced mass of pair $i \neq j$. Note that, for the sake of compact notation, the relative momentum q_k of the free atoms can be formally related to the binding wave number λ_k^D via $q_k = i\lambda_k^D$.

The two-body Schrödinger equation leads to the following two coupled equations ($\nu = 1, 2$):

$$\tilde{\beta}_{k,\nu}(\tilde{E}_{k,\nu} - \tilde{q}_k^2) + \tilde{\Lambda}_{k,\nu}\Theta(E)$$
$$-\frac{\tilde{\Lambda}_{k,\nu}}{2\pi^2}\left(1 + \frac{i\pi}{2}\tilde{q}_k\right)\sum_{\nu'}\tilde{\Lambda}_{k,\nu'}\tilde{\beta}_{k,\nu'} = 0,$$
(5)

where $\Theta(E)$ is the Heaviside step function. In Eq. (5) all quantities are renormalized with respect to the naturally occurring momentum cutoff q_c and its associated energy $E_{c,k} = \hbar^2 q_c^2/2\mu_k$ (see Sec. III B). A dimensionful quantity x is denoted $\tilde{x}$ when normalized.

Solving Eq. (5) for $E > 0$ allows for computation of the scattering amplitude:

$$\tilde{f}(q_k) = -\sum_\nu \frac{\tilde{\Lambda}_{k,\nu}\tilde{\beta}_{k,\nu}}{4\pi}.$$
(6)

The resulting expression is expanded to second order in $\tilde{q}_k$ and compared to the effective range expansion, $\tilde{f}^{-1}(q_k) = -\tilde{a}_k^{-1} - i\tilde{q}_k + \tilde{r}_{e,k}\tilde{q}_k^2/2$, to find the interspecies scattering length $\tilde{a}_k$ and the effective range $\tilde{r}_{e,k}$. When $\tilde{q}_k = 0$ the solution of Eq. (5) leads to an expression of the scattering length which can be directly compared to coupled-channel calculations.

For negative dimer energy $E < 0$, Eq. (5) leads to a fourth-order polynomial equation for λ_k^D, the positive roots of which correspond to the physically relevant solutions [35].

B. Three-body sector

The trimer binding energy $E_T = -\hbar^2\lambda_T^2/2\mu_T$, with $\lambda_T > \max(0, \lambda_k^D)$, is the eigenvalue associated with the three-body wave function:

$$|\psi_{3B}\rangle = \sum_{i,\nu}\int \frac{d^3q}{(2\pi)^3}\beta_{i,\nu}(\vec{q})\hat{b}_{\vec{q},i,\nu}^\dagger\hat{a}_{-\vec{q},i}^\dagger|0\rangle + \int \frac{d^3q_1}{(2\pi)^3}$$
$$\times \int \frac{d^3q_2}{(2\pi)^3}\alpha(\vec{q}_1,\vec{q}_2)\hat{a}_{-\vec{q}_2+\frac{\vec{q}_1}{2},1}^\dagger\hat{a}_{\vec{q}_2+\frac{\vec{q}_1}{2},2}^\dagger\hat{a}_{-\vec{q}_1,3}^\dagger|0\rangle.$$
(7)

Direct substitution of $|\psi_{3B}\rangle$ into $(\hat{H} - E_T)|\psi_{3B}\rangle = 0$ leads to seven coupled integral equations. The first one, from projecting onto the free atom continuum, is

$$\alpha(\vec{q}_1,\vec{q}_2)\left(\frac{\hbar^2|\vec{q}_2 - \frac{\vec{q}_1}{2}|^2}{2m_1} + \frac{\hbar^2|\vec{q}_2 + \frac{\vec{q}_1}{2}|^2}{2m_2} + \frac{\hbar^2 q_1^2}{2m_3} - E_T\right)$$
$$+ \sum_\nu\left[\Lambda_{1,\nu}\beta_{1,\nu}\left(\vec{q}_2 - \frac{\vec{q}_1}{2}\right) + \Lambda_{2,\nu}\beta_{2,\nu}\left(-\vec{q}_2 - \frac{\vec{q}_1}{2}\right) + \Lambda_{3,\nu}\beta_{3,\nu}(\vec{q}_1)\right] = 0.$$
(8a)

The remaining six are structured as three pairs $\nu = 1, 2$:

$$\beta_{1,\nu}(\vec{q}_1)\left(\frac{\hbar^2 q_1^2}{2\mu_1'} + E_{1,\nu} - E_T\right) + \Lambda_{1,\nu}\int \frac{d^3q_2}{(2\pi)^3}\alpha\left(\vec{q}_2 - \frac{\vec{q}_1}{2}, \frac{\vec{q}_2}{2} + \frac{3\vec{q}_1}{4}\right) = 0,$$
(8b)

$$\beta_{2,\nu}(\vec{q}_1)\left(\frac{\hbar^2 q_1^2}{2\mu_2'} + E_{2,\nu} - E_T\right) + \Lambda_{2,\nu}\int \frac{d^3q_2}{(2\pi)^3}\alpha\left(-\vec{q}_2 - \frac{\vec{q}_1}{2}, \frac{\vec{q}_2}{2} - \frac{3\vec{q}_1}{4}\right) = 0,$$
(8c)

$$\beta_{3,\nu}(\vec{q}_1)\left(\frac{\hbar^2 q_1^2}{2\mu_3'} + E_{3,\nu} - E_T\right) + \Lambda_{3,\nu}\int \frac{d^3q_2}{(2\pi)^3}\alpha(\vec{q}_1, -\vec{q}_2) = 0,$$
(8d)

where $\mu_k' = M_i m_i/(M_i + m_i)$ is the reduced mass of the molecule and the free atom.

We note that these equations reduce to the previously derived homonuclear three-channel model for $i = j = k$ and to

the heteronuclear two-channel model in the case $\Lambda_{i,2} = 0$. To proceed, the free particle amplitude $\alpha(\vec{q}_1, \vec{q}_2)$ is eliminated from the first equation and plugged into the others. The first of the two integrals in each equation can be solved, as in the

TABLE I. Parameters of the three-channel model derived from fitting Eq. (9) to coupled-channel calculations of ^{6}Li - ^{133}Cs and using analytic expressions from Ref. [35].

Δ_1/a_0 (G)	1741.13
Δ_2/a_0 (G)	131.351
$B_1 - B_2^{(\mathrm{res})}$ (G)	-68.736
$B_2 - B_2^{(\mathrm{res})}$ (G)	-1.01
$\tilde{\Lambda}_1$	3.50
$\tilde{\Lambda}_2$	0.707

two-body sector, by introducing a high momentum cutoff q_c with which the coupling constants are renormalized according to $\tilde{\Lambda}_{k,\nu} = \Lambda_{k,\nu} q_c^{3/2}/E_c$, and the amplitudes according to $\tilde{\beta}_{k,\nu} = \beta_{k,\nu} q_c^{3/2}$. The renormalized magnetic moment is $\tilde{\mu}_i = \mu_i/E_c$ and all momenta are $\tilde{q} = q/q_c$. In addition one uses the s-wave property that $\beta_{k,\nu}(\vec{q}) = \beta_{k,\nu}(q)$ are spherically symmetric. One thus ends up with six one-dimensional coupled integral equations.

IV. LITHIUM-CESIUM-CESIUM SYSTEM

While Eqs. (8) are too complex to solve in general, they serve as a convenient starting point to study specific cases. Here, we apply the model to the $2 + 1$ case, i.e., two particles with equal masses and one distinguishable particle, of ^{6}Li - ^{133}Cs - ^{133}Cs trimers.

A. Two-body sector

For the remainder of the paper we define the relevant masses: $m = m_{\mathrm{Li}}$ and $M = m_{\mathrm{Cs}}$. In the two-body sector, only one interspecies molecule is possible (LiCs) such that the index k can be omitted in Eq. (5). Solutions of the remaining two equations for $E > 0$ are compared to coupled-channel calculations [36] to fix the free parameters of the model. Here we consider the aa collisional channel of the ^{6}Li - ^{133}Cs mixture, where both atoms are polarized on their respective absolute ground states, and which is relevant for the experiment of Ref. [9]. The two closed channels correspond to the molecules associated with the 843- and 893-G Feshbach resonances.

We proceed in the following way. We fit the magnetic-field dependence of the scattering length provided by coupled-channel calculations with the well-known parametrization expression

$$\tilde{a}_{\mathrm{LiCs}}(B) = \frac{\tilde{\Delta}_1}{B_1^{(\mathrm{res})} - B} + \frac{\tilde{\Delta}_2}{B_2^{(\mathrm{res})} - B}, \qquad (9)$$

where the resonance widths $\tilde{\Delta}_\nu$ and positions $B_\nu^{(\mathrm{res})}$ are experimental observables. These observable parameters are conveniently related to the model's bare parameters via analytic expressions [35] with which the latter are found (see Table I). The differential magnetic moments $\tilde{\mu}_\nu$ are not fitting parameters. Instead, they are extracted from the asymptotic behavior of the coupled-channel dimer binding energies. In real units they are $\mu_1 = -h \times 3.03$ MHz/G and $\mu_2 = -h \times 2.84$ MHz/G.

In Fig. 1(a) the scattering length of the three-channel model as a function of the magnetic field, which by construction
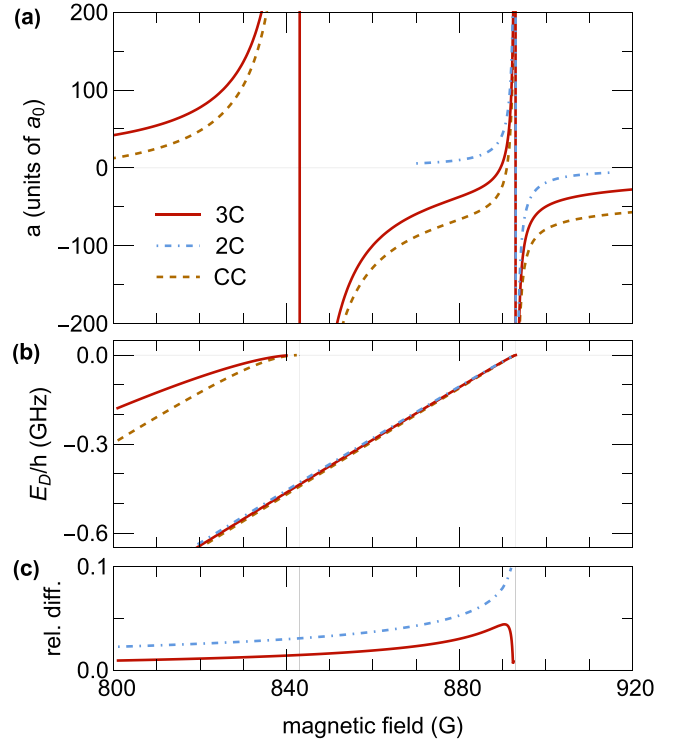

FIG. 1. Two-body sector of LiCs. (a) Magnetic-field dependence of the scattering length, (b) binding energy, and (c) the relative difference of the binding energy. In panels (a) and (b) the dashed brown line corresponds to the coupled-channel calculations and the red solid (blue dash-dotted) line represents the three-channel (two-channel) model. In panel (c) the red solid (blue dashe-dotted) curve shows the binding-energy relative difference between the coupled-channel and the three-channel (two-channel) models. The comparison is shown only for the energy level associated with the narrow Feshbach resonance. The difference with the three-channel model is consistently lower at all magnetic-field values than with the less successful two-channel model.

coincides with Eq. (9), is compared to the coupled-channel calculations together with the result of the two-channel model. The agreement is very good in the vicinity of the Feshbach resonances. The discrepancies between the coupled-channel calculations and the three-channel model are visible for small absolute values of the scattering length. This is because our model does not include the global background scattering length.

To illustrate the success of the model, we compare it with the performance of its simplified version which includes a single closed channel associated with the narrow Feshbach resonance at 893 G. The model is developed along the same lines but keeping only $\nu = 2$ in all expressions in Secs. II and III. To find the bare parameters of the model we fit the coupled-channel calculations with Eq. (9) in the vicinity of the Feshbach resonance while keeping $\tilde{\Delta}_1 = 0$ (see Table II). The fit, also shown in Fig. 1(a), is significantly less successful at capturing the coupled-channel calculations. The absence of the scattering length zero crossing leads to a significant disagreement between the model and the coupled-channel calculations.

TABLE II. Parameters of the two-channel model derived from fitting Eq. (9) (with $\tilde{\Delta}_1 = 0$) to coupled-channel calculations of ^{6}Li-^{133}Cs in the vicinity of the narrow Feshbach resonance at 893 G.

Δ_2/a_0 (G)	132.165
$B_2 - B_2^{(\text{res})}$ (G)	-1.402
$\tilde{\Lambda}_2$	0.673

In Fig. 1(b) the binding energies of the dimers from the coupled-channel calculations are compared to the results of the two- and three-channel model. Both models are successful in describing the narrow resonance and capture the energy level down to hundreds of MHz. However, a closer look at the differences between the models [shown in Fig. 1(c)] emphasizes that the three-channel model is a more successful approach to the real system. The three-channel model also reproduces the binding energy of the intermediate resonance although good agreement is obtained only in the regime of weak binding. This discrepancy might be explained by the intermediate character of the underlying narrow Feshbach resonance for which our model's assumptions ceases to be valid.

In addition, we found the effective range $r_e = -1743a_0$ (at resonance) to differ by 4% from the resonance contribution $-1666\,a_0$ to the effective range. The latter value is found by subtracting the van der Waals contribution $+125\,a_0$ [39] from the coupled-channel value $-1541\,a_0$, which includes the sum of the van der Waals and resonant contributions [40].

In conclusion, the two-body sector reveals that the three-channel model is a better way to describe the real Li-Cs interactions in the aa collisional channel, due to the intermediate Feshbach resonance overlapping with the narrow one and affecting the latter's properties. Adding a third channel is a necessary procedure.

Note that in this particular case there is an alternative theoretical approach. The two-channel model can be extended to include a nonzero background scattering length [41] which is expected to improve the agreement with the coupled-channel

calculations. This approach has its own limitations partially discussed in Ref. [35] and it has not yet been extended to the mass-imbalanced mixtures. The three-channel model is superior because it takes the background scattering length into account by considering its real cause, namely, the presence of another Feshbach resonance in close proximity.

B. Three-body sector

For the LiCsCs three-body sector, Eqs. (8) reduce to four coupled equations. The four remaining molecular amplitudes $\beta_{i,\nu}$ are $i = \{\text{LiCs, CsCs}\}$ and $\nu = \{1, 2\}$.

Further simplifications come from the fact that we neglect Cs-Cs interactions by setting the relevant scattering length (a_{CsCs}) to zero. In reality, its value is moderate and positive in the vicinity of the narrow Feshbach resonance ($a_{\text{CsCs}} = 260a_0$), while it is large and negative at the intermediate resonance ($a_{\text{CsCs}} = -1400a_0$) [42]. Since we consider the Efimov spectrum in the close vicinity of the narrow resonance the latter value is irrelevant. On the other hand, one should be aware of the positive a_{CsCs}, considering the fact that $a_{\text{CsCs}} > 0$ affects the Efimov spectrum measured at intermediate Feshbach resonances [9,27,28]. There, its main influence is to eliminate the ground state of the Efimov spectrum [27,28]. Indeed, also in the vicinity of the narrow resonance, the ground Efimov state was not detected [9]. Additionally, the first excited Efimov resonances in the vicinity of two intermediate resonances were measured to be within $\approx 20\%$ of each other for both positive $a_{\text{CsCs}} = 200a_0$ and large negative $a_{\text{CsCs}} = -1400a_0$ Cs-Cs scattering lengths [9,27]. Thus, $\approx 20\%$ can be considered the upper limit for our error if a_{CsCs} is set to zero. Note, however, that at the narrow resonance, a_{CsCs} is at least an order of magnitude smaller than the absolute values of the effective range and the interspecies scattering length at which the first excited Efimov energy level crosses the threshold. Therefore, its influence on the position of the Efimov resonance is expected to be less important than in the case of intermediate resonances.

This simplification leads to two coupled integral equations for $\beta_{\text{LiCs},\nu} = \beta_\nu$:

$$\left(\frac{\hbar^2 q^2}{2\mu'} + E_\nu - E_T\right)\beta_\nu(q) - \frac{\mu \Lambda_\nu}{\pi^2 \hbar^2}\left(q_c - \frac{\pi}{2}\sqrt{\frac{(2r+1)q^2 + r(r+1)\frac{m}{\mu_T}\lambda_T^2}{(r+1)^2}}\right)\sum_{\nu'}\Lambda_{\nu'}\beta_{\nu'}(q)$$

$$- \frac{m\Lambda_\nu}{4\pi^2\hbar^2}\int_0^\infty dp\,\ln\left(\frac{p^2 + \frac{2r}{r+1}pq + q^2 + \frac{r}{r+1}\frac{m}{\mu_T}\lambda_T^2}{p^2 - \frac{2r}{r+1}pq + q^2 + \frac{r}{r+1}\frac{m}{\mu_T}\lambda_T^2}\right)\sum_{\nu'}\Lambda_{\nu'}\beta_{\nu'}(p) = 0, \tag{10}$$

where $r = M/m$ is the mass ratio and μ_T is the mass of the trimer the definition of which varies throughout the literature. For the sake of convenience in our calculations we define it to be the reduced mass of LiCs. Following the procedure shown in Ref. [35], we choose to extend the integration limit to $-\infty$ and multiply the integral term by $1/2$. Note that this extension requires that both $\beta_1(q)$ and $\beta_2(q)$ be odd functions of q. Then we represent the two three-body amplitudes as a vector, $\psi(q) = [\beta_1(q), \beta_2(q)]^T$, and the coefficients of Eqs. (10)

as a 2×2 matrix, $\mathcal{M}_{\lambda_T}(q_1, q_2)$, that depends on λ_T. Then Eqs. (10) take the form $\int_{-\infty}^\infty dq_2 \mathcal{M}_{\lambda_T}(q_1, q_2)\psi(q_2) = 0$ and a nontrivial solution is obtained for $\det \mathcal{M}_{\lambda_T}(q_1, q_2) = 0$. We perform renormalization as in Sec. III B and use the practical substitution

$$\tilde{q}_i = \sqrt{\frac{r(r+1)}{(2r+1)}\frac{m}{\mu_T}}\tilde{\lambda}\sinh\xi, \tag{11}$$

and Eqs. (10) become

$$\int_{-\infty}^{\infty} d\xi \, \mathcal{M}_{\lambda_T}(\xi, \xi') \psi(\xi') = 0. \tag{12}$$

The vector $\psi(\xi)$ and the matrix elements are

$$\psi(\xi) = [\tilde{\beta}_1(\xi), \tilde{\beta}_2(\xi)]^T, \tag{13a}$$

$$(\mathcal{M}_{\lambda_T})_{ij} = [f_i(\xi')\delta_{ij} - \tilde{\Lambda}_i\tilde{\Lambda}_j g(\xi')]\delta(\xi - \xi') - \tilde{\Lambda}_i\tilde{\Lambda}_j L(\xi, \xi'), \tag{13b}$$

where

$$f_i(\xi) = \tilde{\lambda}_T \cosh \xi + \frac{\tilde{\mu}_i}{\tilde{\lambda}_T \cosh \xi}(B_i - B), \tag{14a}$$

$$g(\xi) = \frac{1}{2\pi^2} \frac{\mu}{\mu_T} \left(\frac{1}{\tilde{\lambda} \cosh \xi} - \frac{\pi}{2} \sqrt{\frac{r}{r+1} \frac{m}{\mu_T}} \right), \tag{14b}$$

$$L(\xi, \xi') = \frac{1}{16\pi^2} \frac{m}{\mu_T} \sqrt{\frac{r(r+1)}{(2r+1)} \frac{m}{\mu_T}} \ln \left(\frac{\sinh^2 \xi' + \frac{2r}{r+1} \sinh \xi' \sinh \xi + \sinh^2 \xi + \frac{(2r+1)}{(r+1)^2}}{\sinh^2 \xi' - \frac{2r}{r+1} \sinh \xi' \sinh \xi + \sinh^2 \xi + \frac{(2r+1)}{(r+1)^2}} \right). \tag{14c}$$

The requirement of a vanishing determinant,

$$\det \mathcal{M}_{\lambda_T}(\xi, \xi') = 0, \tag{15}$$

defines a closed equation for λ_T. In general, there are many values $\lambda_T = \lambda_T^{(\text{sol})}$ for which Eq. (15) is satisfied, however not all of them correspond to physical solutions. To identify the real three-body bound states one must compute the zero-eigenvalue eigenfunction $\psi(\xi)$ of $\mathcal{M}_{\lambda_T^{(\text{sol})}}$ in accordance with Eq. (12) and determine $\tilde{\beta}_1(\xi)$ and $\tilde{\beta}_2(\xi)$. Then, the mathematical solution $\lambda_T^{(\text{sol})}$ is physical only if both are odd functions of ξ. In addition, the number of nodes in $\tilde{\beta}_1(\xi)$ and $\tilde{\beta}_2(\xi)$ allows assignment of $\lambda_T^{(\text{sol})}$ to the ground or an excited Efimov state (see Sec. IV in Ref. [35] for details).

To solve Eq. (15) numerically, each block $\mathcal{M}_{ij}$ is represented as a $n \times n$ matrix by discretizing ξ and ξ' in the interval $[-\xi_m, \xi_m]$ and step size $d\xi = 2\xi_m/(n-1)$. The total matrix thus has dimensions $2n \times 2n$ and its determinant is found. The computed ground and first excited states are shown in Fig. 2, where we used $\xi_m = 20.02$ and $n = 200$ (and $n = 1600$ for some points) together with the parameters of Tables I and II.

V. DISCUSSION AND CONCLUSIONS

In Table III, a comparison between the position of the first excited Efimov resonance predicted by the two- and three-channel models and the experimental result from Ref. [9] is

TABLE III. The experimental value of the resonance position is contrasted to the various theory values. The single-channel Efimov–van der Waals universal theory result is cited as per Table I in Ref. [9].

Source	$a_-^{(2)}(a_0)$
Experiment [9]	$-3330(240)$
Three-channel theory	-3600
Two-channel theory	-7189
Efimov–van der Waals universal theory	-2200

presented. The two-channel model overestimates the position of the resonance by more than a factor of 2. In contrast, the three-channel model agrees quite well with the experimental value. For comparison the Efimov–van der Waals universal theory prediction is also listed. The latter is based on a single-channel model of Refs. [27,43] and cited in Ref. [9]. It is important to emphasize the amazing and not at all obvious fact that the overlapping resonances worked in favor of the experimental observation of the Efimov resonance in this particular case.

Note that our comparison between theory and experiment is limited to the first excited Efimov state. Our minimal model does not capture the absence of the ground state, caused by the finite and positive Cs-Cs scattering length (see discussion in Sec. IV B).

In summary, the results presented in this paper confirm that the Feshbach resonance used in the experiment is narrow
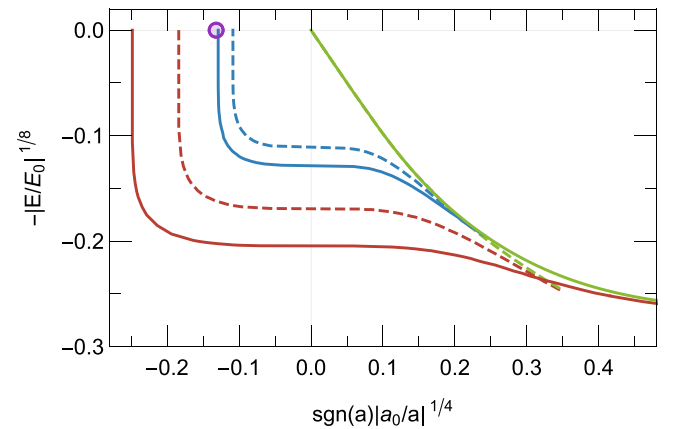

FIG. 2. Three-body sector of LiCsCs. The three-channel model (solid) is compared to the two-channel model (dashed). Shown are the dimer (green) and the ground (red) and first excited (blue) Efimov states. The purple data point is the measurement from Ref. [9]. Here, the normalization energy is $E_0 = \hbar^2/2\mu_T a_0^2$.

enough to effectively decouple the three-body physics from the van der Waals universality. The remaining influence of the van der Waals length can then be estimated to be about 10%. This estimation, however, is within the limits of the above-mentioned conservative error set by the $a_{\text{CsCs}} = 0$ assumption. Therefore, the upper bound for the influence of the finite range of the interaction potential is dominated by the latter, and can thus be quoted as $\lesssim 20\%$.

[1] E. Braaten and H.-W. Hammer, Universality in few-body systems with large scattering length, Phys. Rep. **428**, 259 (2006).

[2] C. H. Greene, P. Giannakeas, and J. Pérez-Ríos, Universal few-body physics and cluster formation, Rev. Mod. Phys. **89**, 035006 (2017).

[3] P. Naidon and S. Endo, Efimov physics: A review, Rep. Prog. Phys. **80**, 056001 (2017).

[4] J. P. D'Incao, Few-body physics in resonantly interacting ultracold quantum gases, J. Phys. B **51**, 043001 (2018).

[5] C. Chin, R. Grimm, P. Julienne, and E. Tiesinga, Feshbach resonances in ultracold gases, Rev. Mod. Phys. **82**, 1225 (2010).

[6] D. S. Petrov, Three-Boson Problem Near a Narrow Feshbach Resonance, Phys. Rev. Lett. **93**, 143201 (2004).

[7] S. Roy, M. Landini, A. Trenkwalder, G. Semeghini, G. Spagnolli, A. Simoni, M. Fattori, M. Inguscio, and G. Modugno, Test of the Universality of the Three-Body Efimov Parameter at Narrow Feshbach Resonances, Phys. Rev. Lett. **111**, 053202 (2013).

[8] R. Chapurin, X. Xie, M. J. Van de Graaff, J. S. Popowski, J. P. D'Incao, P. S. Julienne, J. Ye, and E. A. Cornell, Precision Test of the Limits to Universality in Few-Body Physics, Phys. Rev. Lett. **123**, 233402 (2019).

[9] J. Johansen, B. J. DeSalvo, K. Patel, and C. Chin, Testing universality of Efimov physics across broad and narrow Feshbach resonances, Nat. Phys. **13**, 731 (2017).

[10] J. P. D'Incao and B. D. Esry, Enhancing the observability of the Efimov effect in ultracold atomic gas mixtures, Phys. Rev. A **73**, 030703(R) (2006).

[11] K. Helfrich, H.-W. Hammer, and D. S. Petrov, Three-body problem in heteronuclear mixtures with resonant interspecies interaction, Phys. Rev. A **81**, 042715 (2010).

[12] D. S. Petrov and F. Werner, Three-body recombination in heteronuclear mixtures at finite temperature, Phys. Rev. A **92**, 022704 (2015).

[13] B. Acharya, C. Ji, and L. Platter, Effective-field-theory analysis of Efimov physics in heteronuclear mixtures of ultracold atomic gases, Phys. Rev. A **94**, 032702 (2016).

[14] J. P. D'Incao, M. Krutzik, E. Elliott, and J. R. Williams, Enhanced association and dissociation of heteronuclear Feshbach molecules in a microgravity environment, Phys. Rev. A **95**, 012701 (2017).

[15] P. Giannakeas and C. H. Greene, Ultracold Heteronuclear Three-Body Systems: How Diabaticity Limits the Universality of Recombination Into Shallow Dimers, Phys. Rev. Lett. **120**, 023401 (2018).

[16] D. S. Rosa, T. Frederico, G. Krein, and M. T. Yamashita, Efimov effect in *D* spatial dimensions in *AAB* systems, Phys. Rev. A **97**, 050701(R) (2018).

[17] J. H. Sandoval, F. F. Bellotti, M. T. Yamashita, T. Frederico, D. V. Fedorov, A. S. Jensen, and N. T. Zinner, Squeezing the Efimov effect, J. Phys. B **51**, 065004 (2018).

[18] C.-Y. Zhao, H.-L. Han, M.-S. Wu, and T.-Y. Shi, Universal three-body parameter of heavy-heavy-light systems with a negative intraspecies scattering length, Phys. Rev. A **100**, 052702 (2019).

[19] B. Tran, M. Rautenberg, M. Gerken, E. Lippi, B. Zhu, J. Ulmanis, M. Drescher, M. Salmhofer, T. Enss, and M. Weidemüller, Fermions meet two bosons: The heteronuclear Efimov effect revisited, Braz. J. Phys. **51**, 316 (2021).

[20] P. Giannakeas and C. H. Greene, Asymmetric lineshapes of Efimov resonances in mass-imbalanced ultracold gases, Atoms **9**, 110 (2021).

[21] R. S. Bloom, M.-G. Hu, T. D. Cumby, and D. S. Jin, Tests of Universal Three-Body Physics in an Ultracold Bose-Fermi Mixture, Phys. Rev. Lett. **111**, 105301 (2013).

[22] R. A. W. Maier, M. Eisele, E. Tiemann, and C. Zimmermann, Efimov Resonance and Three-Body Parameter in a Lithium-Rubidium Mixture, Phys. Rev. Lett. **115**, 043201 (2015).

[23] L. J. Wacker, N. B. Jørgensen, D. Birkmose, N. Winter, M. Mikkelsen, J. Sherson, N. Zinner, and J. J. Arlt, Universal Three-Body Physics in Ultracold KRb Mixtures, Phys. Rev. Lett. **117**, 163201 (2016).

[24] K. Kato, Y. Wang, J. Kobayashi, P. S. Julienne, and S. Inouye, Isotopic Shift of Atom-Dimer Efimov Resonances in K-Rb Mixtures: Critical Effect of Multichannel Feshbach Physics, Phys. Rev. Lett. **118**, 163401 (2017).

[25] S.-K. Tung, K. Jiménez-García, J. Johansen, C. Parker, and C. Chin, Geometric Scaling of Efimov States in a ^{6}Li - ^{133}Cs Mixture, Phys. Rev. Lett. **113**, 240402 (2014).

[26] R. Pires, J. Ulmanis, S. Häfner, M. Repp, A. Arias, E. D. Kuhnle, and M. Weidemüller, Observation of Efimov Resonances in a Mixture with Extreme Mass Imbalance, Phys. Rev. Lett. **112**, 250404 (2014).

[27] J. Ulmanis, S. Häfner, R. Pires, E. D. Kuhnle, Y. Wang, C. H. Greene, and M. Weidemüller, Heteronuclear Efimov Scenario with Positive Intraspecies Scattering Length, Phys. Rev. Lett. **117**, 153201 (2016).

[28] S. Häfner, J. Ulmanis, E. D. Kuhnle, Y. Wang, C. H. Greene, and M. Weidemüller, Role of the intraspecies scattering length in the Efimov scenario with large mass difference, Phys. Rev. A **95**, 062708 (2017).

[29] B. Huang, L. A. Sidorenkov, R. Grimm, and J. M. Hutson, Observation of the Second Triatomic Resonance in Efimov's Scenario, Phys. Rev. Lett. **112**, 190401 (2014).

[30] X. Xie, M. J. Van de Graaff, R. Chapurin, M. D. Frye, J. M. Hutson, J. P. D'Incao, P. S. Julienne, J. Ye, and E. A. Cornell,

Observation of Efimov Universality Across a Non-Universal Feshbach Resonance in ^{39}K, Phys. Rev. Lett. **125**, 243401 (2020).

[31] T. Secker, D. J. M. Ahmed-Braun, P. M. A. Mestrom, and S. J. J. M. F. Kokkelmans, Multichannel effects in the Efimov regime from broad to narrow Feshbach resonances, Phys. Rev. A **103**, 052805 (2021).

[32] J.-L. Li, T. Secker, P. M. A. Mestrom, and S. J. J. M. F. Kokkelmans, Strong spin-exchange recombination of three weakly interacting ^{7}Li atoms, Phys. Rev. Research **4**, 023103 (2022).

[33] Y. Castin, Basic theory tools for degenerate Fermi gases, in *Ultra-Cold Fermi Gases, Proceedings of the Enrico Fermi Varenna School on Fermi Gases*, edited by C. Salomon, M. Inguscio, and W. Ketterle (IOS Press, Amsterdam, 2007).

[34] A. O. Gogolin, C. Mora, and R. Egger, Analytical Solution of the Bosonic Three-Body Problem, Phys. Rev. Lett. **100**, 140404 (2008).

[35] Y. Yudkin and L. Khaykovich, Efimov scenario for overlapping narrow Feshbach resonances, Phys. Rev. A **103**, 063303 (2021).

[36] S.-K. Tung, C. Parker, J. Johansen, C. Chin, Y. Wang, and P. S. Julienne, Ultracold mixtures of atomic ^{6}Li and ^{133}Cs with tunable interactions, Phys. Rev. A **87**, 010702(R) (2013).

[37] M. Repp, R. Pires, J. Ulmanis, R. Heck, E. D. Kuhnle, M. Weidemüller, and E. Tiemann, Observation of interspecies ^{6}Li-^{133}Cs Feshbach resonances, Phys. Rev. A **87**, 010701(R) (2013).

[38] J. Ulmanis, S. Häfner, R. Pires, E. D. Kuhnle, M. Weidemüller, and E. Tiemann, Universality of weakly bound dimers and Efimov trimers close to Li-Cs Feshbach resonances, New J. Phys. **17**, 055009 (2015).

[39] B. Gao, Quantum-defect theory of atomic collisions and molecular vibrational spectra, Phys. Rev. A **58**, 4222 (1998).

[40] B. Gao, Analytic description of atomic interaction at ultracold temperatures. II. Scattering around a magnetic Feshbach resonance, Phys. Rev. A **84**, 022706 (2011).

[41] F. Werner, L. Tarruell, and Y. Castin, Number of closed-channel molecules in the BEC-BCS crossover, Eur. Phys. J. B **68**, 401 (2009).

[42] M. Berninger, A. Zenesini, B. Huang, W. Harm, H.-C. Nägerl, F. Ferlaino, R. Grimm, P. S. Julienne, and J. M. Hutson, Feshbach resonances, weakly bound molecular states, and coupled-channel potentials for cesium at high magnetic fields, Phys. Rev. A **87**, 032517 (2013).

[43] Y. Wang, J. P. D'Incao, and B. D. Esry, Ultracold few-body systems, Adv. At. Mol. Opt. Phys. **62**, 1 (2013).